

FIRST RESULTS FROM SPARO: EVIDENCE FOR LARGE-SCALE TOROIDAL MAGNETIC FIELDS IN THE GALACTIC CENTER

G. Novak,¹ D. T. Chuss,¹ T. Renbarger,¹ G. S. Griffin,² M. G. Newcomb,² J. B. Peterson,²
R. F. Loewenstein,³ D. Pernic,³ and J. L. Dotson⁴

ABSTRACT

We have observed the linear polarization of 450 μm continuum emission from the Galactic center, using a new polarimetric detector system that is operated on a 2 m telescope at the South Pole. The resulting polarization map extends ~ 170 pc along the Galactic plane and ~ 30 pc in Galactic latitude, and thus covers a significant fraction of the central molecular zone. Our map shows that this region is permeated by large-scale toroidal magnetic fields. We consider our results together with radio observations that show evidence for poloidal fields in the Galactic center, and with Faraday rotation observations. We compare all of these observations with the predictions of a magnetodynamic model for the Galactic center that was proposed in order to explain the Galactic Center Radio Lobe as a magnetically driven gas outflow. We conclude that the observations are basically consistent with the model.

Subject headings: Galaxy: center — ISM: magnetic fields — polarization

1. Introduction

Beginning with the discovery of the first examples of Galactic center non-thermal filaments (Yusef-Zadeh, Morris, & Chance 1984), radio observers have garnered a steadily growing body of observational evidence pointing toward the existence of large-scale, ordered

¹Department of Physics and Astronomy, Northwestern University, Evanston, IL 60208, g-novak@northwestern.edu

²Department of Physics, Carnegie Mellon University, Pittsburgh, PA 15213

³Yerkes Observatory, University of Chicago, Williams Bay, WI 53191

⁴NASA/Ames Research Center, MS 245-6, Moffett Field, CA 94035

magnetic fields in the Galactic center region, with an overall orientation that is perpendicular to the Galactic plane (Morris 1998). The main tracers of the magnetic field are the Galactic center non-thermal filaments themselves. Such filaments have now been found at a variety of locations throughout the central few hundred pc (LaRosa et al. 2000). They are generally orthogonal to the Galactic plane, and radio polarimetry has confirmed that the magnetic fields in these synchrotron-emitting structures run longitudinally (Lang, Morris, & Echevarria 1999). Diffuse non-thermal emission is also present, but due to Faraday rotation/depolarization, polarimetry of this emission does not always reliably determine the projected field direction. For the few cases where it does, the field turns out to again be perpendicular to the Galactic plane (Tsuboi et al. 1986). This accumulation of radio observations has led to the hypothesis that most of the volume of the Galactic center is permeated by a large-scale magnetic field that is poloidal, or perhaps axial. (Here we are using a cylindrical coordinate system for the Galaxy, and poloidal and axial refer respectively to the component in the r - z plane, and the component along z .) Direct measurements of the strength of this large-scale field do not exist, but it has been argued that it must be of order several mG (Morris 1998).

Along with this relativistic ionized gas, the Galactic center contains a concentration of dense molecular gas, extending ~ 400 pc along the Galactic plane and ~ 50 pc in Galactic latitude (Sofue 1998). Far-infrared and submillimeter polarimetric observations of several flux peaks within this “central molecular zone” have revealed a very wide range of projected magnetic field directions. Overall, these field directions are more nearly parallel to the Galactic plane than perpendicular to it, which has led to the suggestion that the molecular gas is permeated by a toroidal magnetic field rather than a poloidal or axial one (Morris et al. 1992; Novak et al. 2000).

In order to further explore the field in these molecular regions, we have begun a project called SPARO, that has the goal of making a submillimeter polarimetric map covering the entire extent of the central molecular zone. This requires capability for polarimetry of spatially extended, low surface-brightness emission. We achieved this capability by observing at the South Pole, where the skies are exceptionally transparent and stable in the submillimeter (Lane 1998). In this letter we report on the first results of the SPARO project. We describe the observations in § 2, and present our polarimetric map in § 3. In § 4 we discuss our results in the context of a specific model for the Galactic center and its magnetic field.

2. Observations

The observations described here were obtained at the Admundsen-Scott South Pole station, using the SPARO instrument on the Viper telescope. SPARO (the Submillimeter Polarimeter for Antarctic Remote Observations) is a 9-pixel submillimeter array polarimeter incorporating ^3He -cooled detectors (Dotson et al. 1998; Renbarger et al. 2001). Viper is a 2-m diameter Gregorian off-axis telescope, developed primarily for cosmological observations at millimeter and submillimeter wavelengths (Peterson et al. 2000). South Pole Station is inaccessible between February and October of each year, but it is during this “winter” season that submillimeter observing conditions are best. Two of us (G.S.G. and D.P.) remained at South Pole during the winter season of 2000 to operate the SPARO experiment. Observations described here were obtained during April–July 2000.

SPARO’s spectral passband is centered at $\lambda_0 = 450 \mu\text{m}$, with fractional bandwidth $\Delta\lambda/\lambda_0 = 0.10$. The instrument observes simultaneously at 9 sky positions, with the pixels arranged in a 3 by 3 square pattern. The pixel-to-pixel separation is $3.5'$, and the beam FWHM was determined to be $5' \pm 1'$. The lack of bright planets observable from the South Pole during the period of the observations prevented us from determining the beam size more accurately. The pointing accuracy was $\pm 1'$. We used two sky reference positions, separated from the main observing position by $+0.5^\circ$ and -0.5° in cross-elevation, respectively. Moving between main and reference positions was accomplished by rapidly switching the tilt angle of Viper’s flat mirror (at $\sim 3 \text{ Hz}$) while more slowly modulating the telescope’s pointing position (at $\sim 0.01 \text{ Hz}$).

The instrumental polarization was determined by observing the center of the Moon and the peak of Sgr B2 with each pixel. The Moon was assumed to be unpolarized near its center, and the peak of Sgr B2 was assumed to have a polarization of ($P = 0.49\%$; $\phi = 82^\circ$), obtained by averaging $350 \mu\text{m}$ polarimetry results for this source (Dowell et al. 1998) over the area of SPARO’s beam. We estimate that the use of $350 \mu\text{m}$ data to calibrate our $450 \mu\text{m}$ observations introduces an error of only $\sim 0.1\%$ (Dowell et al. 1998; Vaillancourt 2001).

The resulting values for instrumental polarization varied from pixel to pixel but were all in the range 0.3% – 0.6% . Values obtained for a given pixel using the two independent calibrators typically agreed to within $\sim 0.2\%$. We were also able to test for the “non-uniform instrumental polarization” effect (Gonatas et al. 1989), by placing the peak of Sgr B2 at several different locations within the beam of a pixel and looking for changes in the measured polarization. Based on these tests and calibrations, we are confident that the level of systematic error in our polarization measurements is $< 0.3\%$. This translates into an uncertainty in polarization angle of $< (9^\circ)(P/1.0\%)^{-1}$.

3. Results

In Table 1, we present our polarization results with associated statistical errors for sky positions where we obtained polarization detections of statistical significance $P/\sigma_P > 2.75$. Figure 1 shows these results using bar symbols. The orientation of each bar gives the inferred magnetic field direction, that is orthogonal to the E-vector of the measured polarization, and the length of the bar is proportional to the degree of polarization. The bars are superposed on a photometric map that was also obtained using SPARO.

Clearly visible in the photometric map is the large concentration of molecular gas that is associated with the innermost few hundred pc of the Galaxy. (One degree corresponds to 140 pc for an assumed distance of 8.0 kpc.) This concentration of gas is asymmetric, with the highest column density at the position of Sgr B2, displaced toward positive Galactic longitudes from the location of Sgr A* by a projected distance of ~ 100 pc. Our results imply that the magnetic field permeating the Galactic center molecular gas, when projected onto the plane of the sky, is for the most part parallel to the Galactic plane. The simplest explanation for this alignment of projected field direction with Galactic plane is that the molecular gas in the Galactic center is threaded by a large-scale magnetic field having a toroidal (i.e., azimuthal) configuration. This has already been suggested based on previous observations (see § 1), but the SPARO results provide the strongest evidence yet obtained for the existence of this toroidal large-scale field.

4. Discussion

Figure 2 contrasts SPARO results with non-thermal filaments (gray scale) representing evidence for poloidal, or perhaps axial, magnetic fields. Hereafter, in discussing the field traced by the non-thermal filaments, we will use only the more general term, poloidal, to describe the inferred field geometry. It is clear from Figure 2 that the magnetic field in the central few hundred pc is neither purely toroidal nor purely poloidal. Rather, there are regions in which toroidal fields dominate as well as regions in which poloidal fields dominate. However, it is not obvious from this figure how these “toroidal-dominant” and “poloidal-dominant” regions are arranged with respect to one another in three-dimensional space. Furthermore, even when considering the fuller set of observational evidence discussed in § 1, one still cannot unambiguously determine this three-dimensional arrangement.

There does exist a theoretical model for the Galactic center that predicts separate “poloidal-dominant” and “toroidal-dominant” regions within the central few hundred pc. This is the magnetodynamic model developed by Uchida, Shibata, & Sofue (1985, hereafter

USS85), and further refined by Shibata & Uchida (1987). This model was developed in order to explain the “Galactic Center Lobe” (GCL), that is a limb-brightened radio structure with a size of several hundred pc extending from the plane of the Galaxy up towards positive Galactic latitudes (Sofue & Handa 1984). In the model of USS85 the GCL represents a gas outflow that is magnetically driven. The model consists of nonsteady axisymmetric magneto-hydrodynamic simulations in which the field is assumed to be axial at high Galactic latitudes, but acquires a toroidal component near the Galactic plane due to differential rotation of the gas to which it is coupled via flux-freezing. (In the model, the gas density is higher near the plane.) The stress of the resultant magnetic twist is what drives the outflow.

A prediction of this model is that the toroidal component will generally be more dominant for positions nearer to the Galactic plane (Shibata & Uchida 1987). Yusef-Zadeh & Morris (1988) noted that the non-thermal filaments of the Radio Arc (see Figure 2) cross the Galactic plane without showing any bending, thus contradicting this prediction. However, SPARO has now revealed extensive toroidal-dominant regions near the Galactic plane, as predicted by USS85. One way to reconcile Radio Arc observations and SPARO results is to hypothesize that the filaments of the Radio Arc cross the plane at a position where molecular gas is largely absent, and that this is what accounts for the lack of bending. This is plausible because the in-plane areal filling factor of the molecular gas is only about 10% (Bally et al. 1988). Thus the model of USS85 may be correct in an overall sense while failing to predict the detailed structure of the field because it ignores the clumpiness of the gas.

Next, we discuss a third probe of the large-scale field in the Galactic center: Faraday rotation. This effect is produced in thermal gas lying along the line-of-sight to the sources of radio synchrotron emission. The model of USS85 makes a simple prediction for the large-scale distribution of the line-of-sight component of the field. To visualize this prediction, imagine dividing the Galactic center region into four sub-regions (quadrants) according to the signs of the Galactic longitude and Galactic latitude, respectively. For the purposes of this discussion, Galactic longitude and latitude are measured with respect to the true center of the Galaxy at Sgr A*. USS85 then predict that the line-of-sight component should have one sign for the $(+,+)$ and $(-,-)$ quadrants, and the opposite sign for the $(+,-)$ and $(-,+)$ quadrants. The absolute sign of the line-of-sight component is not predicted by the model; only the sign changes between quadrants are predicted. We note that for every point lying within the three-dimensional volume corresponding to a given quadrant, the line-of-sight component of the field has the same sign, according to the model.

USS85 compared this prediction of their model with Faraday rotation observations that were available at that time. Specifically, they considered polarimetry of the “northern plume” and “southern plume”, two extended synchrotron-emitting regions that appear to be, respec-

tively, the Galactic northern and Galactic southern extensions of the non-thermal filaments of the Radio Arc (that are shown in Figure 2). The two plumes extend out to Galactic latitudes of about $+1^\circ$ and -1° , respectively. Faraday rotation measured towards the plumes is believed to be produced in thermal gas located near to the plumes and associated with them. The Faraday rotation measures are predominantly positive for the northern plume, located in the $(+,+)$ quadrant, and predominantly negative for the southern plume, located in the $(+,-)$ quadrant. USS85 noted that such a sign reversal is in agreement with the pattern predicted by their model.

Since the publication of USS85, a handful of observations of Faraday rotation of radiation from individual non-thermal filaments have been made (Lang, Morris, & Echevarria 1999, and references therein). In these cases, the Faraday rotation is due to an extended “Faraday screen” associated with thermal gas in the central ~ 200 pc of the Galaxy. For filaments lying at positive Galactic longitudes, i.e., in the $(+,+)$ and $(+,-)$ quadrants, the sign of the Faraday rotation observed towards the filaments is in good agreement with that observed towards the plumes. Furthermore, we can now use these more recent measurements to explore the line-of-sight field towards negative Galactic longitudes, i.e., in the $(-,+)$ and $(-,-)$ quadrants. Just two measurements have been published for longitudes between 0.0° and -1.0° . Specifically, Yusef-Zadeh, Wardle, & Parastaran (1997) observed negative Faraday rotation measures towards the G359.54+0.18 filament that lies in the $(-,+)$ quadrant, and Gray et al. (1995) found positive rotation measures for the filament known as the “Snake”, that lies in the $(-,-)$ quadrant. Combining these data for the $(-,+)$ and $(-,-)$ quadrants with the pattern already noted by USS85 and given above, namely positive rotation measures in the $(+,+)$ quadrant and negative rotation measures in the $(+,-)$ quadrant, we find that the predicted and observed patterns agree precisely.

We have discussed observations made using three different probes of the magnetic field. The observations are very sparse, and none of them gives direct information on the strength of the field. Field strengths in the Galactic center have been measured using the Zeeman technique (e.g., see Yusef-Zadeh et al. 1999, and Crutcher et al. 1996), but these observations sample relatively small-scale rather than large-scale fields so we have not considered them here. Nevertheless, despite the limitations of the three kinds of magnetic field observations we have discussed, they provide significant evidence in favor of the general picture given by USS85 for the large-scale configuration of the magnetic field in the Galactic center.

For expert technical assistance, crucial help with Antarctic logistics, and invaluable suggestions, we thank J. Carlstrom, D. Dowell, M. Dragovan, P. Goldsmith, J. Hanna, A. Harper, R. Hildebrand, R. Hirsch, J. Jaeger, S. Loverde, P. Malhotra, J. Marshall, H. Moseley, S. Moseley, T. O’Hara, R. Pernic, S. Platt, J. Sundwall, and J. Wirth. The SPARO

project was funded by the Center for Astrophysical Research in Antarctica (an NSF Science and Technology Center; OPP-8920223), by an NSF CAREER Award to G.N. (OPP-9618319), and by a NASA GSRP award to D.C. (NGT5-88). We are grateful to N. E. Kassim, T. N. LaRosa, and D. Pierce-Price for permission to show their data.

REFERENCES

- Bally, J., Stark, A. A., Wilson, R. W., & Henkel, C., 1988, *ApJ*, 324, 223
- Crutcher, R. M., Roberts, D. A., Mehringer, D. M., & Troland, T. H., 1996, *ApJ*, 324, 223
- Dotson, J. L., Novak, G., Renbarger, T., Pernic, D., & Sundwall, J. L., 1998, in *Proceedings of the SPIE 3357, Advanced Technology MMW, Radio, and Terahertz Telescopes*, ed. T. Phillips (Bellingham: SPIE), 543
- Dowell, C. D., Hildebrand, R. H., Schleuning, D. A., Vaillancourt, J. E., Dotson, J. L., Novak, G., Renbarger, T., & Houde, M., 1998, *ApJ*, 504, 588
- Gonatas, D. P., Wu, X. D., Novak, G., & Hildebrand, R. H., 1989, *Appl. Opt.*, 28, 1000
- Gray, A. D., Nicholls, J., Ekers, R. D., & Cram, L. E., 1995, *ApJ*, 448, 164
- Lane, A. P., in *ASP Conf. Ser. 141, Astrophysics from Antarctica*, ed. G. Novak & R. H. Landsberg (San Francisco: ASP), 289
- Lang, C. C., Morris, M., & Echevarria, L., 1999, *ApJ*, 526, 727
- LaRosa, T. N., Kassim, N. E., Lazio, T. J. W., & Hyman, S. D., 2000, *AJ*, 119, 207
- Morris, M., 1998, in *I.A.U. Symp. 184, The Central Regions of the Galaxy and Galaxies*, ed. Y. Sofue (Dordrecht: Kluwer), 331
- Morris, M., Davidson, J. A., Werner, M., Dotson, J., Figer, D. F., Hildebrand, R. H., Novak, G., & Platt, S., 1992, *ApJ*, 399, L63
- Novak, G., Dotson, J. L., Dowell, C. D., Hildebrand, R. H., Renbarger, T., & Schleuning, D. A., 2000, *ApJ*, 529, 241
- Peterson, J. B., Griffin, G. S., Newcomb, M. G., Alvarez, D. L., Cantalupo, C. M., Morgan, D., Miller, K. W., Ganga, K., Pernic, D., & Thoma, M., 2000, *ApJ*, 532, L83.

- Pierce-Price, D., Richer, J. S., Greaves, J. S., Holland, W. S., Jenness, T., Lasenby, A. N., White, G. J., Matthews, H. E., Ward-Thompson, D., Dent, W. R. F., Zylka, R., Mezger, P., Hasegawa, T., Oka, T., Omont, A., & Gilmore, G., 2000, *ApJ*, 545, L121
- Renbarger, T., Chuss, D., Dotson, J. L., Hanna, J. L., Novak, G., Malhotra, P., Marshall, J., Loewenstein, R. F., & Pernic, R., 2001, in preparation
- Shibata, K., & Uchida, Y., 1987, *PASJ*, 39, 559
- Sofue, Y., 1998, in *I.A.U. Symp. 184, The Central Regions of the Galaxy and Galaxies*, ed. Y. Sofue (Dordrecht: Kluwer), 161
- Sofue, Y., & Handa, T., 1984, *Nature*, 310, 568
- Tsuboi, M., Inoue, M., Handa, T., Tabara, H., Kato, T., Sofue, Y., & Kaifu, N., 1986, *AJ*, 92, 818
- Uchida, Y., Shibata, K., & Sofue, Y., 1985, *Nature*, 317, 699
- Vaillancourt, J. E., 2001, *ApJ*, (submitted)
- Yusef-Zadeh, F., & Morris, M., 1988, *ApJ*, 329, 729
- Yusef-Zadeh, F., Morris, M., & Chance, D., 1984, *Nature*, 310, 557
- Yusef-Zadeh, F., Wardle, M., & Parastaran, P., 1997, *ApJ*, 475, L119
- Yusef-Zadeh, F., Roberts, D. A., Goss, W. M., Frail, D. A., & Green, A. J., 1999, *ApJ*, 512, 230

Table 1. Polarization Results

| $\Delta\alpha^a$ | $\Delta\delta^a$ | $P(\%)$ | σ_P | ϕ^b | σ_ϕ |
|------------------|------------------|---------|------------|----------|---------------|
| 23'.1 | 44'.5 | 2.05 | 0.61 | 131.6 | 9.0 |
| 26'.5 | 43'.5 | 1.71 | 0.34 | 116.7 | 6.0 |
| 25'.0 | 40'.0 | 0.67 | 0.14 | 95.8 | 6.5 |
| 28'.2 | 38'.7 | 0.93 | 0.17 | 75.6 | 4.8 |
| 23'.7 | 36'.7 | 0.53 | 0.06 | 88.5 | 3.0 |
| 26'.9 | 35'.4 | 0.96 | 0.13 | 78.3 | 3.4 |
| 19'.1 | 34'.8 | 0.74 | 0.17 | 19.7 | 7.5 |
| 30'.1 | 34'.1 | 1.00 | 0.33 | 76.4 | 8.6 |
| 14'.9 | 32'.7 | 1.35 | 0.43 | 112.9 | 9.0 |
| 25'.6 | 32'.2 | 0.68 | 0.15 | 89.8 | 6.3 |
| 28'.8 | 30'.9 | 1.10 | 0.34 | 93.2 | 8.9 |
| 20'.1 | 26'.8 | 1.99 | 0.60 | 99.1 | 8.4 |
| 15'.5 | 24'.9 | 2.55 | 0.60 | 100.5 | 6.6 |
| 13'.9 | 20'.5 | 2.25 | 0.76 | 124.0 | 9.5 |
| 8'.5 | 17'.0 | 2.13 | 0.54 | 121.7 | 7.2 |
| 8'.0 | 15'.3 | 1.74 | 0.48 | 116.9 | 7.7 |
| 3'.8 | 14'.0 | 1.42 | 0.25 | 103.8 | 4.8 |
| 7'.3 | 12'.8 | 1.08 | 0.22 | 119.7 | 5.8 |
| 10'.5 | 11'.5 | 1.53 | 0.34 | 126.3 | 6.3 |
| 2'.7 | 10'.9 | 1.34 | 0.26 | 114.6 | 5.4 |
| 6'.0 | 9'.6 | 1.02 | 0.22 | 112.7 | 6.4 |
| -5'.2 | 5'.9 | 2.13 | 0.74 | 108.2 | 9.5 |
| -1'.5 | 4'.8 | 0.98 | 0.25 | 116.7 | 7.3 |
| 1'.8 | 3'.5 | 0.73 | 0.18 | 87.6 | 7.2 |
| 0'.5 | 0'.2 | 0.81 | 0.18 | 102.5 | 6.5 |
| 3'.7 | -1'.1 | 1.09 | 0.22 | 103.1 | 5.9 |
| 1'.6 | -1'.4 | 2.22 | 0.49 | 105.4 | 6.3 |
| -4'.5 | -1'.9 | 1.99 | 0.60 | 117.4 | 8.4 |
| -0'.8 | -3'.0 | 1.56 | 0.17 | 118.9 | 3.1 |
| 2'.4 | -4'.3 | 1.57 | 0.21 | 110.6 | 3.8 |
| -7'.1 | -4'.6 | 1.31 | 0.45 | 120.1 | 9.6 |
| -3'.8 | -5'.9 | 0.83 | 0.27 | 117.9 | 9.2 |
| -0'.6 | -7'.2 | 1.53 | 0.27 | 120.8 | 5.1 |
| -8'.4 | -7'.8 | 1.57 | 0.43 | 155.9 | 7.9 |
| -1'.9 | -10'.5 | 2.00 | 0.31 | 116.2 | 4.5 |
| -6'.4 | -12'.4 | 2.31 | 0.40 | 122.8 | 4.9 |
| -3'.2 | -13'.7 | 1.48 | 0.36 | 119.5 | 6.7 |

^aOffsets in Right Ascension and Declination are measured relative to the position of Sgr A*.

^b ϕ is the angle of the E-vector of the polarized radiation, measured in degrees from north-south, increasing counterclockwise.

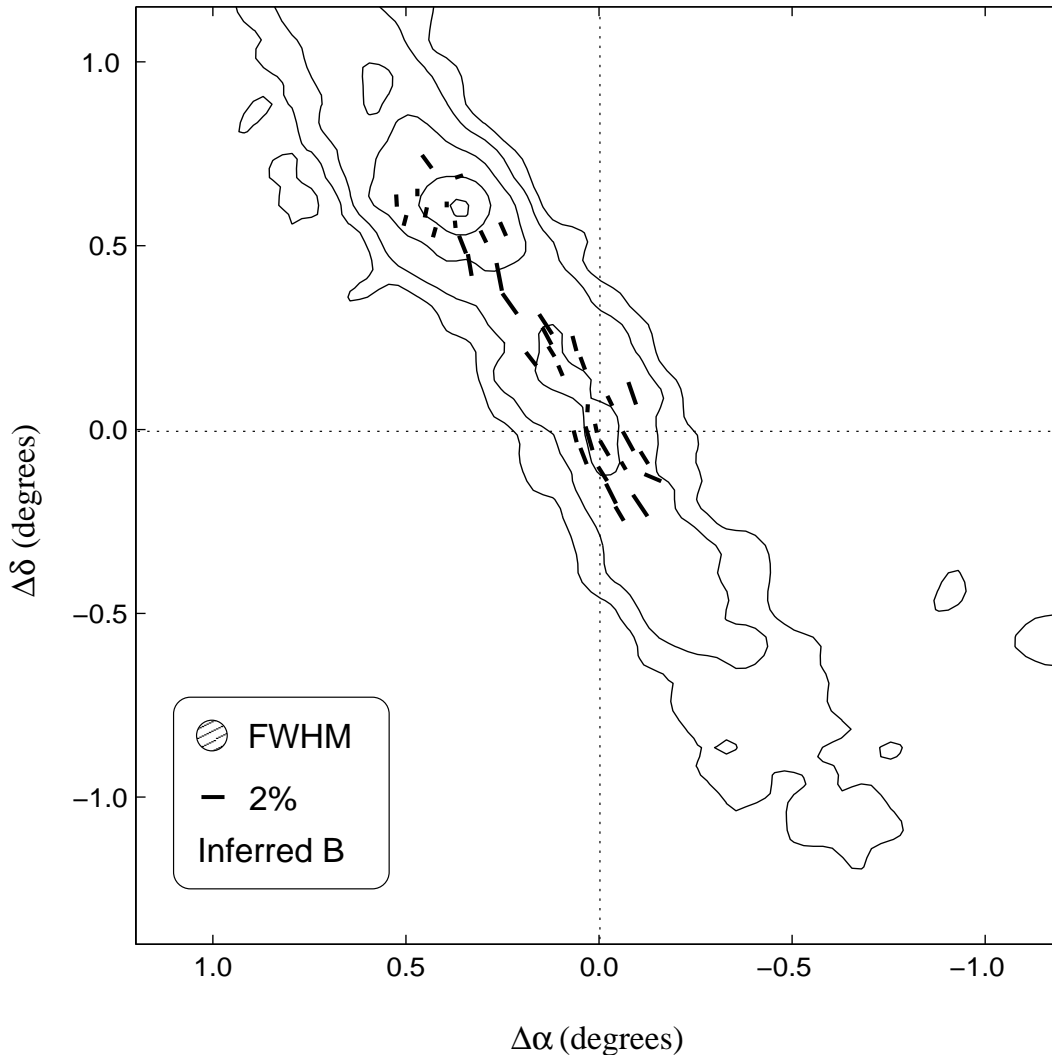


Fig. 1.— Results of $450\ \mu\text{m}$ polarimetry (bars) and photometry (contours) of the Galactic center, obtained using SPARO. The distribution of $450\ \mu\text{m}$ flux closely follows the Galactic plane, that lies at a position angle of $+31^\circ$. Coordinate offsets are measured with respect to the location of Sgr A* (that lies at the intersection of the horizontal and vertical dotted lines). Each bar is drawn parallel to the inferred magnetic field direction (i.e. perpendicular to the E-vector of the measured submillimeter polarization), and the length of the bar indicates the measured degree of polarization (see key at bottom left). Contours are drawn at 0.075, 0.15, 0.30, 0.60, and 0.95 times the peak flux, which is located at the position of Sgr B2. For clarity, negative contours are not shown. The reference beam offsets were the same for polarimetry and photometry and are given in § 2. The $5'$ beam of SPARO is shown in the key. Positive Galactic latitudes lie towards the upper right of the figure, and positive Galactic longitudes lie towards upper left.

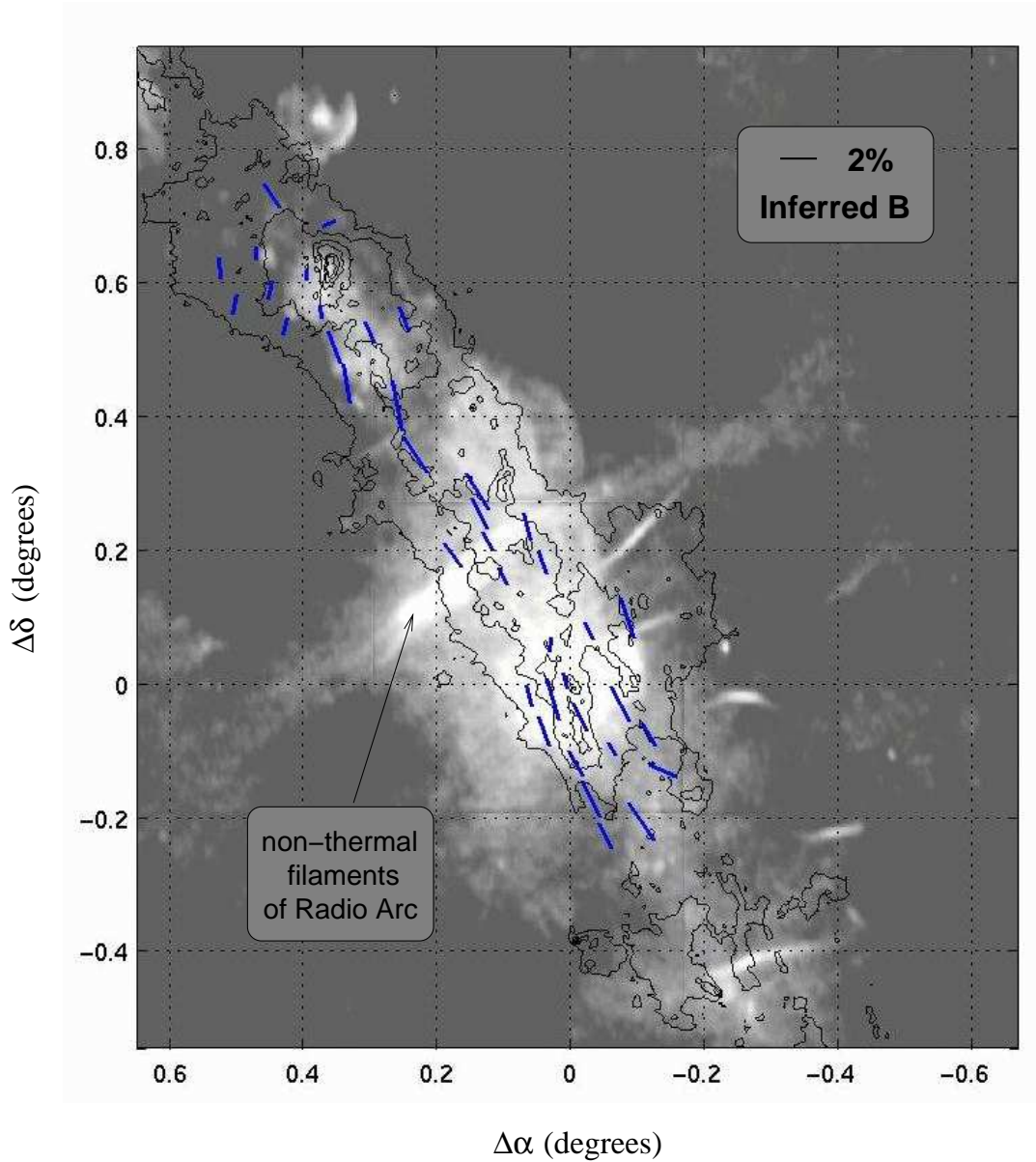


Fig. 2.— 450 μm polarization measurements (bars) shown together with 90 cm radio continuum image (gray scale, LaRosa et al. 2000), and 850 μm continuum emission (contours, Pierce-Price et al. 2000). As in Fig. 1, the orientation of each bar is parallel to the inferred magnetic field direction (i.e., orthogonal to the measured direction of polarization) and its length is proportional to the degree of polarization. The radio continuum image shows about six locations where non-thermal filaments can be seen. These non-thermal filaments trace magnetic fields in hot ionized regions (see § 1). The gray scale image is logarithmically scaled, and the contours of 850 μm emission are also logarithmic. Coordinate offsets are measured with respect to the position of Sgr A*. The location of the brightest bundle of non-thermal filaments (referred to as the non-thermal filaments of the Radio Arc) is indicated in the figure.